Mathematical Modeling and Numerical Simulations for Drug Release from PLGA Particles *

Yu Sun[1], Yan Li[2], and Jiangguo Liu[3]

[1] School of Advanced Materials Discovery (SAMD), Colorado State University, Fort Collins, CO 80523, USA, sundaym@rams.colostate.edu
[2] Department of Design & Merchandising and SAMD, Colorado State University, Fort Collins, CO 80523, USA, yan.li@colostate.edu
[3] Department of Mathematics and SAMD, Colorado State University, Fort Collins, CO 80523-1874, USA, liu@math.colostate.edu

Abstract. Poly lactic-co-glycolic acid (PLGA) is a copolymer that has demonstrated great potentials in development of novel drug delivery systems. This paper first discusses synthesis procedures and properties of PLGA micro/nanoparticles (MPs/NPs) and then examine mechanisms of drug release from PLGA particles. For the core-shell structure of reservoir-type PLGA MPs/NPs, diffusion through the polymeric shell is identified as the main mechanism of drug release. A time-dependent diffusion equation is used to model release from homogeneous spherical particles. Finite volume schemes are developed for the radial diffusion model. Numerical results and *in vitro* experiment data are discussed.

Keywords: Core-shell structure · Diffusion · Drug release · Finite volume schemes · Microparticles and nanoparticles · PLGA (poly lactic-co-glycolic acid)

1 Introduction

Polymers have been used in the pharmaceutical industry for several decades due to their biocompatible, biodegradable, and nontoxic properties [1,3,5,7,9,19,22]. A considerable amount of research has been devoted to the roles of poly-lactic-co-glycolic-acid (PLGA), poly-ethylene-oxide (PEO), and polyethylene glycol (PEG) in drug delivery. PLGA has shown great potentials in making drug delivery systems. It was approved by FDA as a material for therapeutic devices due to its biocompatibility and biodegradability [2,10,15,24]. After PLGA is introduced to human metabolism system, it can decompose into carbon dioxide and water, causing no harm to human bodies.

PLGA can be formed into particles at the micro- or nano-meter level and various shapes, e.g., slabs, cylinders, or spheres with therapeutic agents (drugs) encapsulated. The drugs will be released later in a controlled manner. Applications

* Y. Sun and J. Liu were partially supported by US National Science Foundation under grant DMS-2208590.

ICCS Camera Ready Version 2023
To cite this paper please use the final published version:
DOI: 10.1007/978-3-031-36030-5_28

of PLGA MPs/NPs for control of bacterial infection and cures of Alzheimer's disease and breast cancer can be found in [2,10,15].

Four major mechanisms and three main release stages have been identified for drug release from PLGA micro- or nano-particles [16,17,18].

- Diffusion through the polymeric shell;
- Convection through the pores in the polymeric shell;
- Osmotic pumping;
- Degradation.

Diffusion is the major mechanism observed in the early stage [14].

Development of mathematical models for drug release from porous polymer systems dates back to the early 1980s, see [6] and references therein. Back then, the focus was on finding series solutions and then approximation for short-time behaviors, usually under the perfect sink condition, see [12] and references therein. Effects of variable boundary conditions and distribution of particle size on release behaviors were also investigated [12]. For diffusion-controlled release from reservoir or matrix systems, a summary of the series solutions was given in [14] for slabs, cylinders, and spheres. This approach is still very useful as demonstrated in a recent work [4] using series expansion in terms of eigenfunctions to investigate drug delivery from a multilayer spherical capsule. Finite element methods were investigated in [20,23] for diffusional drug release from complex matrix systems. All these demonstrate that mathematical models are helpful for design of new drug delivery systems [11].

The rest of this paper is organized as follows. Section 2 briefly describes a procedure for synthesis of PLGA particles and how drug, e.g., gentamicin, is encapsulated into PLGA MPs/NPs. Section 3 discusses properties of PLGA particles and commonly observed release mechanisms of drug release from PLGA MPs/NPs. Section 4 examines mathematical modeling for drug release from PLGA particles. Section 5 develops a numerical method for the radial diffusion equation that models release from spherical particles with the core-shell structure. Section 6 discusses numerical results and experimental data. The paper is concluded with some remarks in Section 7.

2 Synthesis of PLGA Particles and Drug Encapsulation

Various techniques have been used in preparation of PLGA MPs/NPs and encapsulation of drugs [3,7,10,22]. Gentamicin is a commonly used drug being encapsulated in PLGA particles. This is finished through a synthesis procedure based on a double emulsion evaporation method [16]. Different solutions for emulsion are prepared first. These include, for instance,

- 100 mg PLGA dissolved in 6 ml dichloromethane (DCM) as the oil phase;
- 20 mg gentamicin dissolved in water as the aqueous phase 1;
- 12% PVA solution as the aqueous phase 2.

ICCS Camera Ready Version 2023
To cite this paper please use the final published version:
DOI: 10.1007/978-3-031-36030-5_28

The synthesis procedure contains 4 steps.

(i) Oil phase (PLGA/DCM) was mixed with aqueous phase 1 (gentamicin/water), yielding a primary emulsion solution;
(ii) Sonication was applied to the mixture for 3 minutes with a 35% amplitude;
(iii) Double-emulsion nano-droplets were formed via mixing primary emulsion solution with aqueous phase 2 (PVA/water);
(iv) The double-emulsion nano-droplet solution was allowed to evaporate for 6 hours, then PLGA NPs precipitated.

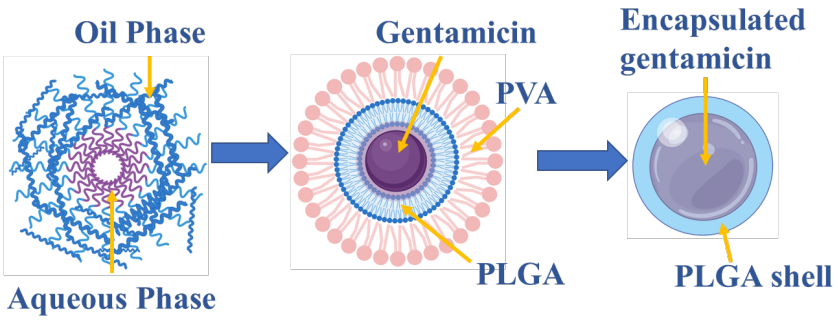

Fig. 1. An illustration of synthesis of PLGA micro-/nano-particles and encapsulation of drug gentamicin.

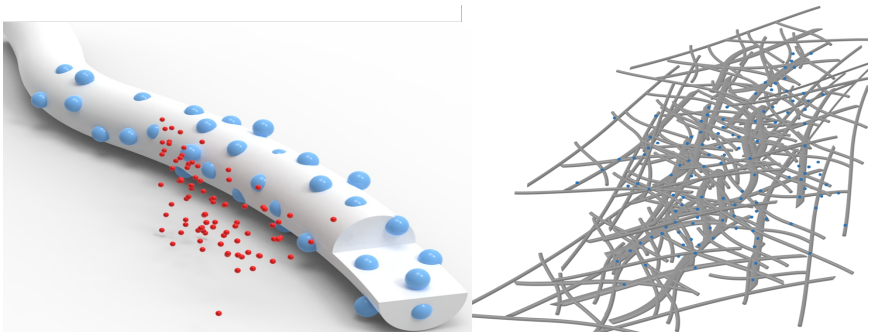

Fig. 2. An illustration of drug gentamicin being encapsulated in PLGA nanoparticles (PU-PEO nanofiber scaffolds).

Electron-spinning is an effective way to incorporate NPs into fibers. Solutions of 0.35g PU dissolved in 10ml DCM and 0.2g PEO dissolved in 10ml DCM are prepared first. Then PU and PEO solution were mixed with PLGA NP solutions for 10-minute sonication to yield an emulsion solution. A scanning electron

ICCS Camera Ready Version 2023
To cite this paper please use the final published version:
DOI: 10.1007/978-3-031-36030-5_28

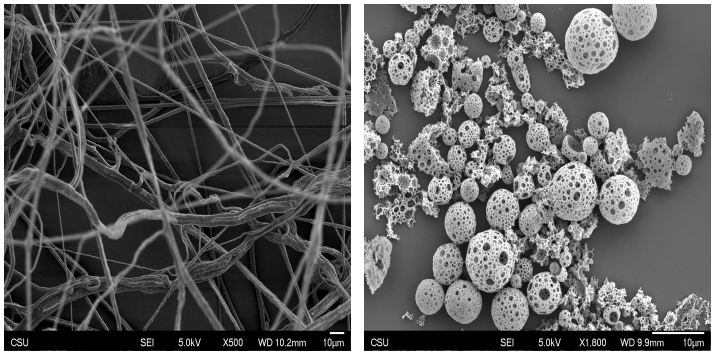

Fig. 3. *Left panel*: A scanning electron microscopy (SEM) image of gentamicin-encapsulated PLGA NPs with PU-PEO fiber; *Right panel*: An SEM image of PLGA NPs with porous shells.

microscopy (SEM) image of gentamicin-encapsulated PLGA NPs is shown in Figure 3. The core-shell structure and porous shells can be clearly observed.

3 Properties of PLGA Particles and Release Mechanisms

With the synthesis procedure discussed in Section 2, PLGA particles are mostly in the spherical shape, as shown in Figure 3 right panel. Shown in Figure 4 is a distribution of the diameters of PLGA particles from a particular experiment when the PLGA concentration was at 16.7 mg/ml.

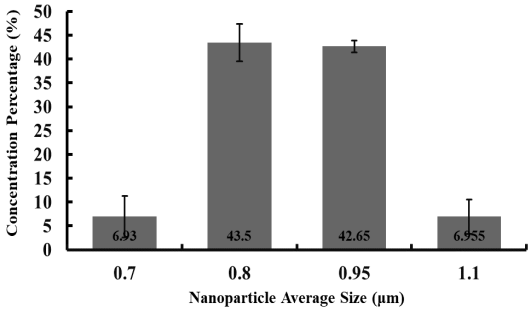

Fig. 4. Size (diameter) distribution of PLGA particles from an *in vitro* experiment.

A summary of PLGA particles average size, thickness, number of PLGA MPs/NPs and estimated loading gentamicin concentration is given in Table 1.

Major mechanisms of drug release from PLGA particles, as listed in Table 2 have been identified in the literature [16,17,18]. An illustration of the major

ICCS Camera Ready Version 2023
To cite this paper please use the final published version:
DOI: 10.1007/978-3-031-36030-5_28

Table 1. Properties of PLGA particles & drug gentamicin observed in five experiments

PLGA/DCM concentration (mg/ml)	Yield rate (%)	Average diameter (μm)	Thickness (μm)	PLGA NPs (#)	Gentamicin initial concentration (mg/ml)
13.3	68.34%	1.5	0.21	5.78×10^7	0.0768
15.0	58.89%	1.6	0.48	3.58×10^7	0.0621
16.7	96.33%	1.0	0.06	4.77×10^8	0.0177
18.3	32.12%	1.8	0.17	6.19×10^7	0.0297
20.0	38.16%	2.4	0.20	3.18×10^7	0.0224

Table 2. Summary of drug release mechanisms from PLGA particles

Mechanisms	**Description**
Diffusion thru polymeric shell	Early stage of release process, burst effect
Convection thru pores	Through the pores in the polymeric shell
Osmotic pumping	Due to concentration gradient
Degradation	Degradation of NPs

mechanisms in the process of drug release from PLGA particles is also provided in Figure 5.

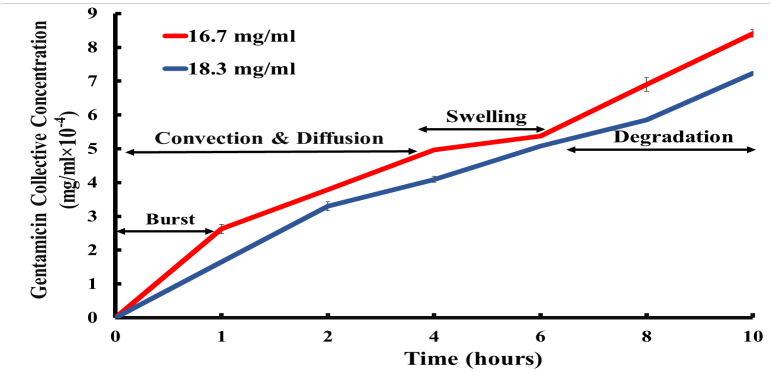

Fig. 5. An illustration of major mechanisms for drug release from PLGA particles.

4 Mathematical Modeling for Drug Release from PLGA Particles

4.1 A Model for Radial Diffusion in Polymeric Shells

We follow the approaches and major assumptions in [14]. Specifically,

ICCS Camera Ready Version 2023
To cite this paper please use the final published version:
DOI: 10.1007/978-3-031-36030-5_28

(i) PLGA MPs/NPs are formed as reservoir devices for drug delivery;
(ii) The drug solution inside the core is a *constant activity resource*;
(iii) The PLGA MPs/NPs have a core-shell structure, in particular, the inner and outer radii are r_a, r_b;
(iv) The polymeric shell is porous and homogeneous, drug is diffused through this shell, the diffusivity is a positive constant D;
(v) For the early stage of the diffusion process, the drug concentration at the inner membrane (r_a) is maintained as a constant.

Shown in Figure 6 is an illustration of the spherical core-shell structure of a typical PLGA particle.

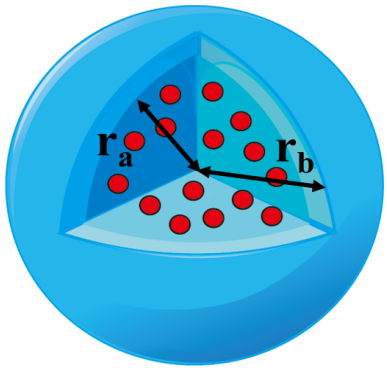

Fig. 6. An illustration of the spherical core-shell structure of typical PLGA particles.

Based on Fick's 2nd law [13,14], we write down a time-dependent diffusion equation in the radial direction with a constant diffusivity as below.

$$\begin{cases} \dfrac{\partial c}{\partial t} = \dfrac{D}{r^2}\dfrac{\partial}{\partial r}\left(r^2\dfrac{\partial c}{\partial r}\right), \quad r \in [r_a, r_b],\ t \in (0, T] \\ \text{Boundary conditions} \\ \text{Initial condition} \end{cases} \tag{1}$$

For the above simple model, the early work focused on finding series solutions. For a special case with a constant initial condition and a constant Dirichlet boundary condition, see [12] for a series solution. [14] summarized the classical work up to Year 2012 and provided a nice overview of various models of dosage forms and their series solutions.

As *in vitro* experiments for investigation of drug-release from PLGA particles are expensive and vary with lab conditions, the *in silico* approach with numerical simulations will offer meaningful alternative/supplementary data to experiment reslts. This relies on accurate and efficient numerical methods for solving the differential equation boundary initial value problems.

ICCS Camera Ready Version 2023
To cite this paper please use the final published version:
DOI: 10.1007/978-3-031-36030-5_28

4.2 Other Existing Mathematical Models

There exist a good number of mathematical models for drug release from PLGA or more generally polymeric devices, depending on what mechanisms are being considered, e.g., diffusion, convection, swelling, and degradation. The popular ones are the 0th order, 1st order, Higuchi, and Korsmeyer-Peppas models, according to `ChatGPT`.

The Peppas equation shown below applies to non-swellable matrix systems in the early stage [11,12]:

$$\frac{M_t}{M_\infty} = A\, t^\beta, \tag{2}$$

where M_t is the accumulative mass of the drug released up to time t, M_∞ is the total mass released up to time infinity, A, β are positive constants. In particular, $\beta = 0.50$ for slabs, $\beta = 0.45$ for cylindrical particles, $\beta = 0.43$ for spherical particles. It is also mentioned that, if $0.50/0.45/0.43 < \beta < 1.00$, the diffusion is anomalous, i.e., non-Fickian. This simple exponential relation was elaborated in [12] and further justified in [11].

For drug release from non-swellable polymeric devices (reservoir or matrix), a summary of mathematical models can be found in [14]. In particular, for a spherical particle of the reservoir type with a core-shell structure under the assumption of constant activity source, there holds

$$M_t = 4\pi D K c_s \frac{r_b r_a}{r_b - r_a} t, \tag{3}$$

where D is the drug diffusivity, K is a drug partition parameter, c_s is the solubility concentration, r_a, r_b are the inner and outer radii, respectively, and t is time. See [14] p.355. We will fit our experimental data with this model later.

5 Numerical Methods for Radial Diffusion

In this section, we develop efficient numerical schemes for solving the radial diffusion equation that models drug diffusion through the polymeric shell of sphere-shaped PLGA particles.

5.1 Node-oriented Finite Volume Schemes for Spherical Diffusion

In this subsection, we develop numerical schemes for the spherical diffusion problem, which shares some features with the control volume method in [21]. We consider a constant radial diffusion equation with a source term

$$\frac{\partial u}{\partial t} = \frac{D}{r^2}\frac{\partial}{\partial r}\Big(r^2 \frac{\partial u}{\partial r}\Big) + f(r,t), \tag{4}$$

which can be rewritten as

$$r^2 \frac{\partial u}{\partial t} + \frac{\partial}{\partial r}\Big(- D \frac{\partial u}{\partial r} r^2\Big) = r^2 f(r,t). \tag{5}$$

ICCS Camera Ready Version 2023
To cite this paper please use the final published version:
DOI: 10.1007/978-3-031-36030-5_28

Let $0 < r_a < r_b$ be the inner and outer radii of a spherical shell. Consider a uniform partition $r_a = r_1 < \cdots < r_n = r_b$ with $h = (r_b - r_a)/(n-1)$ being the mesh size. For node r_i, we consider the control volume $[r_i - \frac{h}{2}, r_i + \frac{h}{2}]$. This will be a half volume when $i = 1$ or $i = n$.

Integrating Equation (5) LHS 1st term over the control volume, we obtain

$$\int_{r_{i-\frac{1}{2}}}^{r_{i+\frac{1}{2}}} \frac{\partial u}{\partial t} r^2 dr = \frac{\partial}{\partial t}\Big(\int_{r_{i-\frac{1}{2}}}^{r_i} u\, r^2 dr + \int_{r_i}^{r_{i+\frac{1}{2}}} u\, r^2 dr \Big). \tag{6}$$

Consider the integrand $w(r) = r^2\, u(r,t)$ in the above integrals. We approximate its derivatives in the half volumes $[r_{i-\frac{1}{2}}, r_i]$ and $[r_i, r_{i+\frac{1}{2}}]$, respectively, to obtain

$$w'(r_i) \approx \frac{r_i^2 u_i - r_{i-1}^2 u_{i-1}}{h}, \qquad w'(r_i) \approx \frac{r_{i+1}^2 u_{i+1} - r_i^2 u_i}{h}. \tag{7}$$

The Taylor expansion in these two half volumes takes the forms shown below.

$$\begin{aligned} w(r) = r^2\, u &= r_i^2 u_i + (r - r_i)\frac{r_i^2 u_i - r_{i-1}^2 u_{i-1}}{h} + \mathcal{O}(h^2), \\ w(r) = r^2\, u &= r_i^2 u_i + (r - r_i)\frac{r_{i+1}^2 u_{i+1} - r_i^2 u_i}{h} + \mathcal{O}(h^2). \end{aligned} \tag{8}$$

Plugging these back into Equation (6) yields

$$\int_{r_{i-\frac{1}{2}}}^{r_{i+\frac{1}{2}}} \frac{\partial u}{\partial t} r^2 dr = h\, \frac{\partial}{\partial t}\Big(\frac{1}{8} r_{i-1}^2 u_{i-1} + \frac{6}{8} r_i^2 u_i + \frac{1}{8} r_{i+1}^2 u_{i+1} + \mathcal{O}(h^2) \Big). \tag{9}$$

Similar formulas can be established for the half volumes related to $i = 1, n$.

Now we check the diffusion term on the LHS of Equation (5). The integral is treated by the Fundamental Theorem of Calculus and cancellation.

$$\begin{aligned} \int_{r_{i-\frac{1}{2}}}^{r_{i+\frac{1}{2}}} D \frac{\partial}{\partial r}\Big(r^2 \frac{\partial u}{\partial r} \Big) dr &= D \int_{r_{i-\frac{1}{2}}}^{r_i} \frac{\partial}{\partial r}\Big(r^2 \frac{\partial u}{\partial r} \Big) dr + D \int_{r_i}^{r_{i+\frac{1}{2}}} \frac{\partial}{\partial r}\Big(r^2 \frac{\partial u}{\partial r} \Big) dr \\ &= D\, r_{i+\frac{1}{2}}^2 \frac{\partial u}{\partial r}\Big|_{r_{i+\frac{1}{2}}} - D\, r_{i-\frac{1}{2}}^2 \frac{\partial u}{\partial r}\Big|_{r_{i-\frac{1}{2}}} \\ &= \frac{D}{h}\Big(r_{i-\frac{1}{2}}^2 u_{i-1} - \Big(r_{i-\frac{1}{2}}^2 + r_{i+\frac{1}{2}}^2 \Big) u_i + r_{i+\frac{1}{2}}^2 u_{i+1} \Big) + \mathcal{O}(h^2). \end{aligned} \tag{10}$$

As for the two special cases $i = 1, n$, one has, respectively,

$$\begin{aligned} \int_{r_1}^{r_{\frac{3}{2}}} D \frac{\partial}{\partial r}\Big(r^2 \frac{\partial u}{\partial r} \Big) &\approx \frac{D}{h}\Big(-(r_{\frac{3}{2}}^2 - r_1^2) u_1 + (r_{\frac{3}{2}}^2 - r_1^2) u_2 \Big) \\ \int_{r_{n-\frac{1}{2}}}^{r_n} D \frac{\partial}{\partial r}\Big(r^2 \frac{\partial u}{\partial r} \Big) &\approx \frac{D}{h}\Big(-(r_n^2 - r_{n-\frac{1}{2}}^2) u_{n-1} + (r_n^2 - r_{n-\frac{1}{2}}^2) u_n \Big). \end{aligned} \tag{11}$$

ICCS Camera Ready Version 2023
To cite this paper please use the final published version:
DOI: 10.1007/978-3-031-36030-5_28

For the RHS of Equation (5), we use the midpoint quadrature to obtain

$$\int_{r_{i-\frac{1}{2}}}^{r_{i+\frac{1}{2}}} f r^2 dr = h r_i^2 f_i + \mathcal{O}(h^3), \quad 2 \le i \le (n-1). \tag{12}$$

For the special cases $i = 1$ and $i = n$, we have

$$\int_{r_1}^{r_{\frac{3}{2}}} f r^2 dr \approx \frac{h}{2} r_1^2 f_1, \quad \int_{r_{n-\frac{1}{2}}}^{r_n} f r^2 dr \approx \frac{h}{2} r_n^2 f_n. \tag{13}$$

Let $\mathbf{v}(t) = \big[v_1(t), v_2(t), \cdots, v_n(t)\big]^T$ be the dim-n column vector consisting of the numerical solution nodal values. We obtain an ODE system

$$\mathbf{M}\frac{d\mathbf{v}}{dt} + \mathbf{S}\,\mathbf{v} = \mathbf{g}, \tag{14}$$

where $\mathbf{S}$ and $\mathbf{M}$ are the stiffness and mass matrices, respectively.

$$\mathbf{S} = \frac{D}{h}\begin{bmatrix} r_{\frac{3}{2}}^2 - r_1^2 & -(r_{\frac{3}{2}}^2 - r_1^2) & \cdots & \cdots & \cdots \\ \cdots & \cdots & \cdots & \cdots & \cdots \\ \cdots & -r_{i-\frac{1}{2}}^2 & r_{i-\frac{1}{2}}^2 + r_{i+\frac{1}{2}}^2 & -r_{i+\frac{1}{2}}^2 & \cdots \\ \cdots & \cdots & \cdots & \cdots & \cdots \\ \cdots & \cdots & \cdots & r_n^2 - r_{n-\frac{1}{2}}^2 & -(r_n^2 - r_{n-\frac{1}{2}}^2) \end{bmatrix}, \tag{15}$$

$$\mathbf{M} = \frac{h}{8}\begin{bmatrix} 3r_1^2 & r_2^2 & 0 & 0 & \cdots & 0 & 0 & 0 \\ r_1^2 & 6r_2^2 & r_3^2 & 0 & \cdots & 0 & 0 & 0 \\ 0 & r_2^2 & 6r_3^2 & r_4^2 & \cdots & 0 & 0 & 0 \\ \cdots & \cdots & \cdots & \cdots & \cdots & \cdots & \cdots & \cdots \\ 0 & 0 & 0 & 0 & \cdots & r_{n-2}^2 & 6r_{n-1}^2 & r_n^2 \\ 0 & 0 & 0 & 0 & \cdots & 0 & r_{n-1}^2 & 3r_n^2 \end{bmatrix}. \tag{16}$$

Note that vector $\mathbf{g}$ corresponds to the source term.

The linear ODE system in (14) can be solved using the implicit Euler or Crank-Nicolson methods. Let $\Delta t = T/m$ and $0 = t_0 < \cdots < t_{j-1} < t_j < \cdots < t_m = T$ be a uniform temporal partition. Let $\mathbf{v}^{(j)}$ be the fully discretized numerical solution at time t_j. Then the implicit Euler discretization yields

$$\mathbf{M}\frac{\mathbf{v}^{(j+1)} - \mathbf{v}^{(j)}}{\Delta t} + \mathbf{S}\,\mathbf{v}^{(j+1)} = \mathbf{g}^{(j+1)}, \tag{17}$$

and hence

$$(\mathbf{M} + \Delta t\,\mathbf{S})\mathbf{v}^{(j+1)} = \mathbf{M}\,\mathbf{v}^{(j)} + \Delta t\,\mathbf{g}, \quad j = 0, 1, \cdots, (m-1). \tag{18}$$

ICCS Camera Ready Version 2023
To cite this paper please use the final published version:
DOI: 10.1007/978-3-031-36030-5_28

After modification by boundary conditions, the above linear system can be solved by a standard linear solver. This offers a well-defined time-marching scheme.

For better approximation accuracy of the numerical solution, we could also use the Crank-Nicolson discretization

$$\mathbf{M}\frac{\mathbf{v}^{(j+1)}-\mathbf{v}^{(j)}}{\Delta t}+\mathbf{S}\frac{1}{2}\left(\mathbf{v}^{(j+1)}+\mathbf{v}^{(j)}\right)=\frac{1}{2}\left(\mathbf{g}^{(j+1)}+\mathbf{g}^{(j)}\right), \tag{19}$$

which leads to another time-marching scheme,

$$\left(\mathbf{M}+\frac{\Delta t}{2}\mathbf{S}\right)\mathbf{v}^{(j+1)}=\left(\mathbf{M}-\frac{\Delta t}{2}\mathbf{S}\right)\mathbf{v}^{(j)}+\frac{\Delta t}{2}\left(\mathbf{g}^{(j+1)}+\mathbf{g}^{(j)}\right), \tag{20}$$

for $j=0,1,\cdots,(m-1)$.

5.2 Computation of Mass and Fluxes

For the above numerical schemes, we can compute (mass) fluxes at the two radial ends r_a and r_b, which correspond to the interior and exterior shells for the core-shell structure of spherical PLGA MPs/NPs.

At a typical time moment $t_j(j=0,1,\cdots,m)$, the numerical solution $v^{(j)}(r)$ is a continuous piecewise linear polynomial determined by its nodal values. The numerical total mass in the radial interval $[r_a,r_b]$ is, by direct calculations,

$$\begin{aligned}M_j&=\sum_{i=1}^{n-1}\int_{r_i}^{r_{i+1}}v^{(j)}(r)r^2dr=\int_{r_i}^{r_{i+1}}\left(v_i^{(j)}\frac{r_{i+1}-r}{h}+v_{i+1}^{(j)}\frac{r-r_i}{h}\right)r^2dr\\&=\sum_{i=1}^{n-1}\left(v_i^{(j)}r_{i+1}-v_{i+1}^{(j)}r_i\right)\frac{1}{3h}(r_{i+1}^3-r_i^3)\\&+\sum_{i=1}^{n-1}\left(v_{i+1}^{(j)}-v_i^{(j)}\right)\frac{1}{4h}(r_{i+1}^4-r_i^4),\quad j=0,1,\cdots,m.\end{aligned} \tag{21}$$

The outflow fluxes at r_b and r_a, (for $j=1,2,\cdots,m$) are respectively,

$$\begin{aligned}F_j^b&=-\frac{D}{2}\left(\frac{v_{N_r}^{(j)}-v_{N_r-1}^{(j)}}{h}+\frac{v_{N_r}^{(j-1)}-v_{N_r-1}^{(j-1)}}{h}\right)r_b^2\,\Delta t,\\F_j^a&=\frac{D}{2}\left(\frac{v_2^{(j)}-v_1^{(j)}}{h}+\frac{v_2^{(j-1)}-v_1^{(j-1)}}{h}\right)r_a^2\,\Delta t.\end{aligned} \tag{22}$$

Since there is no source in this case, mass conservation for the numerical solution takes the following form

$$M_j-M_{j-1}=F_j^a+F_j^b,\quad j=1,\cdots,m. \tag{23}$$

ICCS Camera Ready Version 2023
To cite this paper please use the final published version:
DOI: 10.1007/978-3-031-36030-5_28

5.3 Nondimensionalization

The numerical solvers discussed in the previous subsection could produce simulation results for release from single PLGA particle once the model parameters, e.g., diffusivity D, the inner and outer radii r_a, r_b, are provided. For units of parameters or variables, we follow [4]. See Table 3.

Table 3. Units of parameters/variables for spherical diffusion

Variables	Units	Meaning
D	$cm^2\, s^{-1}$	Diffusion coefficient
c	mg/ml	Concentration
r_a, r_b, r	cm	Radial positions
t	s	Time

For better performance of numerical simulations, we introduce new dimensionless parameters and variables $\hat{D}, \hat{r}, \hat{t}, \hat{c}$ so that

$$\widehat{D} = \frac{D}{D_0}, \qquad \widehat{t} = \frac{t}{T_0}, \qquad \widehat{r} = \frac{r}{r_b}, \qquad \widehat{c} = \frac{c}{C_0}, \tag{24}$$

where D_0, T_0, C_0 are chosen according to experiment data. Let $H_0 = (r_b - r_a)/r_b$ be the thickness of the polymeric shell. Then the nondimensionalized diffusion problem takes the form

$$\begin{cases} \dfrac{\partial \widehat{c}}{\partial \widehat{t}} = \dfrac{T_0 D_0}{r_b^2} \dfrac{\widehat{D}}{\widehat{r}^2} \dfrac{\partial}{\partial \widehat{r}} \left(\widehat{r}^2 \dfrac{\partial \widehat{c}}{\partial \widehat{r}} \right), \quad \widehat{r} \in [1 - H_0, 1],\ \widehat{t} \in (0, 1], \\ \text{Boundary conditions}, \\ \text{Initial condition}. \end{cases} \tag{25}$$

The source term does not exist for drug release from PLGA particles.

6 Experimental and Numerical Results

Note that *in vitro* experiment data vary. For our experiments gentamicin encapsulated in PLGA particles, three sets of radii are recorded as follows.
– Case 1: $r_a = 0.7\,\mu m = 7.0 * 10^{-5} cm$, $r_b = 0.8\,\mu m = 8.0 * 10^{-5} cm$;
– Case 2: $r_a = 0.8\,\mu m = 8.0 * 10^{-5} cm$, $r_b = 1.0\,\mu m = 1.0 * 10^{-5} cm$;
– Case 3: $r_a = 1.8\,\mu m = 1.8 * 10^{-4} cm$, $r_b = 2.0\,\mu m = 2.0 * 10^{-4} cm$.
This indicates the relative thickness $H_0 = (r_b - r_a)/r_b$ is in the range $0.10 - 0.20$. The observation time T_0 could be chosen as 1hr – 2 hrs, namely, 3600 – 7200 seconds, to focus on the early (burst) stage.

The diffusivity parameter D is difficult to obtain. An empirical formula was proposed in [13] based on data fitting and knowledge from series solutions of

ICCS Camera Ready Version 2023
To cite this paper please use the final published version:
DOI: 10.1007/978-3-031-36030-5_28

similar problems. For the *in silico* approach, one may consider a baseline value for D_0 and vary it up or down for several magnitudes in numerical simulations.

For our five *in vitro* experiments with gentamicin encapsulated in PLGA particles, we record the accumulative percentage of gentamicin released versus time. As shown in Table 4, about 20% of total gentamicin was released after about 2 hours; about 60% of total gentamicin was released after about 10 hours.

Table 4. Accumulative percentage of gentamicin release in five experiments

PLGA/DCM (mg/ml) concentration	13.30	15.0	16.7	18.3	20.0
Time (hours)	Accumulative % of gentamicin released				
1	11.54%	12.86%	15.77%	9.92%	9.41%
2	21.71%	22.29%	22.73%	19.82%	17.92%
4	26.03%	28.15%	29.81%	24.56%	23.51%
6	31.04%	31.68%	32.25%	30.47%	30.88%
8	36.11%	37.99%	41.43%	35.09%	33.58%
10	44.34%	46.11%	50.46%	43.37%	42.97%

The raw data suggests that we should focus on the 1st hour for a potential stage of burst. Following the discussion in [14] Fig.4, we fit the model "reservoir devices with constant activity source" (Eqn.(7) therein) using our experimental data for the 1st 60 min with 2-min sampling. Linear regression yields

$$M_t = 4.2 * 10^{-3}\, t. \tag{26}$$

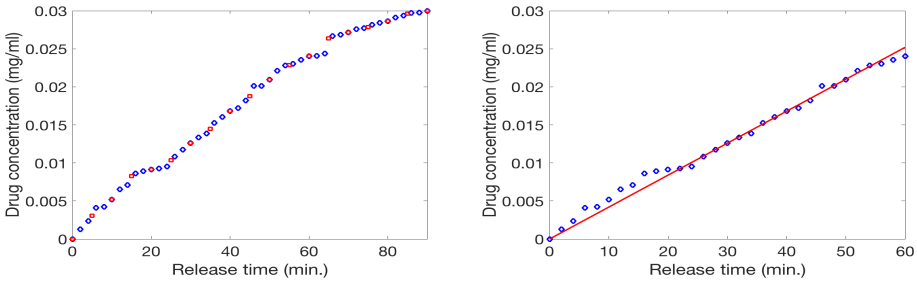

(a) $\diamond$ for 2m samples, $*$ for 5m samples (b) Red line for the fitted model

Fig. 7. Experimental data fitting for gentamicin release from PLGA particles. (a) Raw data showing the accumulative oncentration of released drug during the 1st 90 minutes; (b) The red line represents the fitting model $M_t = 4.2 * 10^{-3}\, t$ for $t \in [0, 60]$ min.

ICCS Camera Ready Version 2023
To cite this paper please use the final published version:
DOI: 10.1007/978-3-031-36030-5_28

7 Concluding Remarks

This paper investigates mathematical modeling and numerical simulations for drug release from PLGA particles as our exploratory efforts in this interdisciplenary approach. Based on examination of data obtained from *in vitro* experiments, our focus is placed on modeling the early stage of release with assumptions of *no swelling of the porous shell*, *homogeneity of the shell*, and *the perfect sink condition*, a radial direction diffusion equation is adopted. Finite volume schemes have been developed for this model. `Matlab` code modules along with *in silico* results will be incorporated in our code package `DarcyLite` [8].

Due to the pores on the polymeric shells of PLGA MPs/NPs, a time-dependent convection-diffusion equation would be more suitable for modeling the drug release process. This is currently under our investigation and will be reported in our future work.

As drug release proceeds, the porous shell is subject to swelling and eventually degrades. Mathematical modeling and numerical simulations for degradation are more challenging. These are under our investigation also.

Simulations of drug release from PLGA MPs/NPs using Molecular Dynamics (MD) seem too expensive and hence will not be our pursuit. Our goal is to develop efficient simulation code modules that can run on laptop or low-configuration desktop computers. These code modules will be based on the mathematical equations that characterize transport through porous media.

References

1. Busatto, C., Pesoa, J., Helbling, I., Luna, J., Estenoz, D.: Effect of particle size, polydispersity and polymer degradation on progesterone release from PLGA microparticles: Experimental and mathematical modeling. Int. J. Pharm. **536**, 360–369 (2018)
2. Delbreil, P., Rabanel, J.M., Banquy, X., Brambilla, D.: Therapeutic nanotechnologies for Alzheimer's disease: A critical analysis of recent trends and findings. Adv. Drug Deliv. Rev. **187**, 114397 (2022)
3. Ghitman, J., Biru, E.I., Stan, R., Iovu, H.: Review of hybrid PLGA nanoparticles: Future of smart drug delivery and theranostics medicine. Mater. Dsgn. **193**, 108805 (2020)
4. Jain, A., McGinty, S., Pontrelli, G., Zhou, L.: Theoretical model for diffusion-reaction based drug delivery from a multilayer spherical capsule. Int. J. Heat Mass Trans. **183**, 122072 (2022)
5. Jusu, S.M., Obayemi, J., Salifu, A., Nwazojie, C., Uzonwanne, V., odusanya, O., Soboyejo, W.: Drug-encapsulated blend of PLGA-PEG microspheres: in vitro and in vivo study of the effects of localized/targeted drug delivery on the treatment of triple-negative breast cancer. Sci. Rep. **10**, 14188 (2020)
6. Korsmqer, R.W., Gumy, R., Doelker, E., Buri, P., Peppas, N.A.: Mechanisms of solute release from porous hydrophilic polymers. Int. J. Pharm. **15**, 25–35 (1983)
7. Lagreca, E., Onesto, V., Natale, C.D., Manna, S.L., Netti, P.A., Vecchione, R.: Recent advances in the formulation of PLGA microparticles for controlled drug delivery. Prog. Biomat. **9**, 153–174 (2020)

ICCS Camera Ready Version 2023
To cite this paper please use the final published version:
DOI: 10.1007/978-3-031-36030-5_28

8. Liu, J., Sadre-Marandi, F., Wang, Z.: DarcyLite: A Matlab toolbox for Darcy flow computation. Proc. Comput. Sci. **80**, 1301–1312 (2016)
9. Naghipoor, J., Rabczuk, T.: A mechanistic model for drug release from PLGA-based drug eluting stent: A computational study. Comput. Bio. Med. **90**, 15–22 (2017)
10. Operti, M.C., Bernhardt, A., Grimm, S., Engel, A., Figdor, C.G., Tagit, O.: Plga-based nanomedicines manufacturing: Technologies overview and challenges in industrial scale-up. Int. J. Pharm. **605**, 120807 (2021)
11. Peppas, N.A., Narasimhan, B.: Mathematical models in drug delivery: How modeling has shaped the way we design new drug delivery systems. J. Con. Rel. **190**, 75–81 (2014)
12. Ritger, P.L., Peppas, N.A.: A simple equation for description of solute release I. Fickian and non-Fickian release from non-swellable devices in the form of slabs, spheres, cylinders or discs. J. Con. Rel. **5**, 23–36 (1987)
13. Siepmann, J., Elkharraz, K., Siepmann, F., Klose, D.: How autocatalysis accelerates drug release from PLGA-based microparticles: A quantitative treatment. Biomacromol. **6**, 2312–2319 (2005)
14. Siepmann, J., Siepmann, F.: Modeling of diffusion controlled drug delivery. J. Con. Rel. **161**, 351–362 (2012)
15. Su, Y., Zhang, B., Sun, R., Liu, W., Zhu, Q., Zhang, X., Wang, R., Chen, C.: PLGA-based biodegradable microspheres in drug delivery: recent advances in research and application. Drug Deliv. **28**, 1397–1418 (2021)
16. Sun, Y., Bhattacharjee, A., Reynolds, M., Li, Y.V.: Synthesis and characterizations of gentamicin-loaded poly-lactic-co-glycolic (PLGA) nanoparticles. J. Nanopart. Res. **23**, 155 (2021)
17. Tamani, F., Bassand, C., Hamoudi, M.C., Siepmann, F., Siepmann, J.: Mechanistic explanation of the (up to) 3 release phases of PLGA microparticles: Monolithic dispersions studied at lower temperatures. Int. J. Pharm. **596**, 120220 (2021)
18. Tamani, F., Bassand, C., Hamoudi, M., Danede, F., Willart, J., Siepmann, F., Siepmann, J.: Mechanistic explanation of the (up to) 3 release phases of PLGA microparticles: Diprophylline dispersions. Int. J. Pharm. **572**, 118819 (2019)
19. Tamani, F.: Towards a better understanding of the drug release mechanisms in PLGA microparticles. Ph.D. thesis, Université de Lille, France (2019)
20. Wu, X., Zhou, Y.: Finite element analysis of diffusional drug release from complex matrix systems. II. factors influencing release kinetics. J. Con. Rel. **51**, 57–71 (1998)
21. Zeng, Y., Albertus, P., Klein, R., Chaturvedi, N., Kojic, A., Bazant, M.Z., Christensen, J.: Efficient conservative numerical schemes for 1d nonlinear spherical diffusion equations with applications in battery modling. J. Electrochem. Soc. **160**(9), A1565–A1571 (2013)
22. Zhou, J., Zhai, Y., Xu, J., Zhou, T., Cen, L.: Microfluidic preparation of PLGA composite microspheres with mesoporous silica nanoparticles for finely manipulated drug release. Int. J. Pharm. **593**, 120173 (2021)
23. Zhou, Y., Wu, X.: Finite element analysis of diffusional drug release from complex matrix systems. I. complex geometries and composite structures. J. Con. Rel. **49**, 277–288 (1997)
24. Zhu, X., Braatz, R.D.: Modeling and analysis of drug-eluting stents with biodegradable PLGA coating: Consequences on intravascular drug delivery. J. Biomech. Eng. **136**, 111004 (2014)

ICCS Camera Ready Version 2023
To cite this paper please use the final published version:
DOI: 10.1007/978-3-031-36030-5_28